REVIEW / SYNTHÈSE

New perceptions of transcription factor properties from NMR

Stefan Bagby, Cheryl H. Arrowsmith, and Mitsuhiko Ikura

Abstract: The complementarity of NMR and X-ray crystallography for biomacromolecular studies has been particularly evident in analysis of transcription factor structures and interactions. While X-ray crystallography can be used to tackle relatively complicated structural problems including multicomponent (three and higher) complexes, NMR studies have provided new insights into the nature of protein–DNA and protein–protein interactions that would be difficult to obtain by other biophysical methods. We describe herein some of the novel and important information recently derived from NMR studies of transcription factors.

Key words: protein–DNA interaction, protein–protein interaction, induced folding, conformational fluctuations, transcriptional regulation.

Résumé : La complémentarité de la RMN et de la cristallographie par rayons X pour les études de macromolécules biologiques est particulièrement évidente dans le cas de l'étude de la structure et des interactions des facteurs de transcription. Alors que la cristallographie par rayons X peut être utilisée pour étudier des problèmes structuraux relativement compliqués, comme les complexes ayant trois constituants ou plus, la RMN permet d'obtenir de nouvelles informations concernant la nature des interactions protéine–ADN et protéine–protéine qu'il serait difficile d'obtenir par d'autres méthodes biophysiques. Dans cet article, nous décrivons quelques-unes des nouvelles informations importantes obtenues récemment grâce à l'étude de facteurs de transcription à l'aide de la RMN.

Mots clés : interaction protéine–ADN, interaction protéine–protéine, repliement induit, fluctuations de conformation, régulation de la transcription.

[Traduit par la Rédaction]

Introduction

NMR spectroscopy and X-ray crystallography are the two principal techniques for obtaining atomic resolution structures of biomacromolecules. In addition to the three-dimensional structures of many DNA-binding domains (DBDs) and some protein–DNA complexes (Billeter et al. 1993; Chuprina et al. 1993; Foster et al. 1997; Huth et al. 1997; Love et al. 1995; Ogata et al. 1994; Omichinski et al. 1993, 1997; Werner et al. 1995, 1997; Zhang et al. 1994; Zhou et al. 1998), NMR studies have provided unique insights into transcription factor properties. Much of this novel information arises from the capacity of NMR to probe the dynamic characteristics of proteins and their macromolecular complexes across a wide range of frequencies and includes (*i*) an appreciation of the coupling of local protein folding and protein–DNA or protein–protein interaction, (*ii*) an appreciation of the dynamic nature of the protein–DNA interface, (*iii*) an appreciation of the role of hydration water in the dynamic protein–DNA interface, and (*iv*) an improved understanding of the spatial and motional relationship between domains of multidomain transcription factors.

Below we discuss the recent studies that have produced these new insights and end with an account of recently exploited sources of structural information that permit elucidation of long range order by NMR. These new methods are

Received April 20, 1998. Revised July 6, 1998. Accepted July 9, 1998.

Abbreviations: *Antp*(*C39S*), mutant *Antennapedia* homeodomain (Cys-39 replaced by Ser); DBD, DNA-binding domain; $dTAF_{II}230$, *Drosophila* $TAF_{II}230$; *lac* HP56, *lac* repressor headpiece residues 1–56; NOE, nuclear Overhauser enhancement; RIR, Rel insert region; TBP, TATA box binding protein; TFIIBc, carboxy-terminal core domain of human TFIIB (residues 112–316); TFIIBn, N-terminal fragment of human TFIIB (residues 1–60); zf1–3, first three zinc fingers of TFIIIA from *Xenopus laevis* oocytes.

S. Bagby, C.H. Arrowsmith, and M. Ikura.[1] Division of Molecular and Structural Biology, Ontario Cancer Institute, and Department of Medical Biophysics, University of Toronto, 610 University Avenue, Toronto, ON M5G 2M9, Canada.

[1]Author to whom all correspondence should be addressed (e-mail: mikura@oci.utoronto.ca).

Table 1. Local folding processes for protein–DNA interactions identified from NMR studies.

Protein	Folding process coupled with DNA binding*
trp repressor	Increased helical content in helix-turn-helix motif
Glucocorticoid receptor	Folding of Zn-finger motif and dimerization
GCN4 basic leucine zipper	Folding of basic region from coil to helix
Gal4	Helix formation and dimerization via coiled-coil interactions
Ant homeodomain	Disordered N-terminal residues (1–6) become ordered and interact with the DNA minor groove
NFAT	Two loops become ordered, including formation of a helix, at DNA binding surface of protein

* See text for citations.

particularly suited to the study of protein–DNA complexes among other systems.

Coupling of local folding and sequence-specific DNA binding

Comparison of the solution NMR structures of a variety of DBDs with the corresponding high-resolution crystal structures of the protein–DNA complexes has revealed a common theme in protein–DNA interactions: very often the solution structure of the unbound DBD contains less secondary, tertiary, and (or) quaternary structure than the protein conformation in the crystal structure (and NMR structure when available) of the protein–DNA complex. The importance of NMR in revealing this coupling of local folding with DNA binding is underscored by the fact that the increased disorder observed for the unbound proteins in solution is often not seen in crystal structures of the free proteins, possibly because of the lower temperatures used to collect X-ray crystallographic data or the stabilizing effects of crystal packing.

Transcription factors that take on additional structure in the DNA-bound state (Table 1) include *Antennapedia* homeodomain (Kissinger et al. 1990; Qian et al. 1989), *Escherichia coli trp* repressor (Arrowsmith et al. 1991; Otwinowski et al. 1988; Zhao et al. 1993), yeast GAL4 (Baleja et al. 1992; Kraulis et al. 1992; Marmorstein et al. 1992) (Fig. 1), yeast GCN4 (Ellenberger et al. 1992; Saudek et al. 1991) and the basic leucine zipper family (Pathak and Sigler 1992), *Drosophila* GAGA (Omichinski et al. 1997), the glucocorticoid receptor DBD (Härd et al. 1990; Luisi et al. 1991), and human NFATC1 (Wolfe et al. 1997; Zhou et al. 1998). With the notable exception of NFATC1, most of these proteins have predominantly α-helical DNA-binding domains that have increased helical content upon binding DNA.

The core DNA recognition domain of NFATC1 provides an excellent example of induced local folding and its implications for transcriptional regulation. NFATC1 DBD adopts an antiparallel β-barrel fold that is structurally related to s-type domains of the immunoglobulin superfamily. Relaxation measurements on free NFATC1 DBD show that two large surface loops are disordered. These loops become ordered in the NFATC1–DNA complex: one of them, corresponding to the Rel insert region (RIR), includes a short α-helix and both are directly involved in protein–DNA interaction (Fig. 2). This induced folding orders two residues in the RIR that are important for cooperative interaction with another transcription factor, AP-1, in the NFAT–AP-1–DNA ternary complex (Sun et al. 1997). Induced structure in NFATC1 DBD is therefore important for both protein–DNA and protein–protein interactions.

It has been proposed that this coupling of local folding with DNA binding is a general feature of protein–DNA interactions and that it can be considered as an allosteric effect of DNA on the protein(s) (Lefstin and Yamamoto 1998). Spolar and Record (1994) pointed out that the degree of local folding (which can vary from limited to extensive) correlates with the negative changes in heat capacity that accompany these binding reactions. The higher degree of disorder revealed by the NMR studies therefore reflects an important thermodynamic property of DNA-binding proteins in solution, rather than a shortcoming in the precision of the NMR technique relative to X-ray crystallography.

Domains involved in transcriptional regulation: coupling of local folding and protein–protein interaction

Evidence derived from NMR and other biophysical studies indicates that transcriptional activation domains are typically largely unstructured in aqueous solution at neutral pH (Cho et al. 1996; Dahlman-Wright et al. 1995; Donaldson and Capone 1992; Lienhard Schmitz et al. 1994; Van Hoy et al. 1993). Some activation domains may be induced to adopt α-helical conformations (Dahlman-Wright et al. 1995; Donaldson and Capone 1992; Lienhard Schmitz et al. 1994; McEwan et al. 1996) and others to adopt β-strand conformations (Van Hoy et al. 1993) using hydrophobic solvents or acidic conditions. More recently, it has been demonstrated using NMR that local folding of a transactivation domain can occur upon interaction with a structured polypeptide target. For example, Verdine and coworkers (Uesugi et al. 1997) used transfer nuclear Overhauser effect (NOE) experiments to show that the minimal activation domain of the herpes simplex virus VP16 protein undergoes an induced transition from random coil to α-helix upon interaction with one of its targets, human $TAF_{II}31$. The phosphorylated kinase-inducible domain (pKID) of the CREB transactivation domain also undergoes a coil-to-helix transition upon interaction with the KIX domain of the coactivator CBP (Radhakrishnan et al. 1997). pKID forms two helices, of which an amphipathic helix makes most of the interactions with KIX. The N-terminal region of *Drosophila* $TAF_{II}230$ undergoes a more complex induced folding process upon interaction with the TATA box

Fig. 1. Induced structural changes accompanying DNA interaction by the DNA-binding domain (residues 1–65) of the *Saccharomyces cerevisiae* transcriptional activator GAL4. (Left) The ensemble of NMR-derived structures of the free form (Baleja et al. 1992) and (right) the X-ray crystallographic structure of the DNA-bound form (Marmorstein et al. 1992) of GAL4 DNA-binding domain. The yellow spheres represent metal ions (cadmium was used in both free and DNA complex structures, but zinc is the physiological metal ligand). One monomer of the DNA-bound dimer is red, the other is blue. The N- and C-termini of the displayed polypeptides are labelled. The region corresponding to the parallel coiled coil dimerization element (residues 50–64) is disordered in the absence of DNA (left) such that the free DNA-binding domain is monomeric. This figure was prepared using Molscript (Kraulis 1991) and rendered using Raster3D (Merritt and Bacon 1997).

binding protein (TBP) to form a compact domain comprising three α-helices and a β-hairpin (Liu et al. 1998). The TBP binding surface of $dTAF_{II}230$ mimics the TATA element surface, providing the structural basis of the mechanism by which $dTAF_{II}230$ inhibits TBP interaction with the TATA element. In these last two instances, NMR methods were used to determine the full three-dimensional structures of the pKID:KIX (Radhakrishnan et al. 1997) and TBP–$dTAF_{II}230$ complexes (Liu et al. 1998).

Conformational fluctuations at the protein–DNA interface

TFIIIA

NMR has been used to provide the first direct structural analysis of a TFIIIA–DNA complex through a study of the structure and dynamics of the first three zinc fingers of TFIIIA (zf1–3) in complex with a 15 base pair oligonucleotide corresponding to the TFIIIA recognition site on the 5S RNA gene (Foster et al. 1997). TFIIIA contains nine zinc fingers (Ginsberg et al. 1984; Miller et al. 1985), but zf1–3 is sufficient for specific, high-affinity DNA binding. Each of the three fingers comprises a helix packed against a small β-hairpin. Protein–DNA contacts are made predominantly by residues in the helix and at the fingertip. Fingers 2 and 3 lie along the major groove and finger 1 lies across the major groove.

The NMR characteristics of lysine side chains involved in conferring sequence specificity on TFIIIA–DNA interaction suggest that the side chains fluctuate between contacts with different bases rather than making discrete contacts. Lys-26 and Lys-29 of finger 1 are proximal to highly negatively charged regions and can potentially form a hydrogen bond

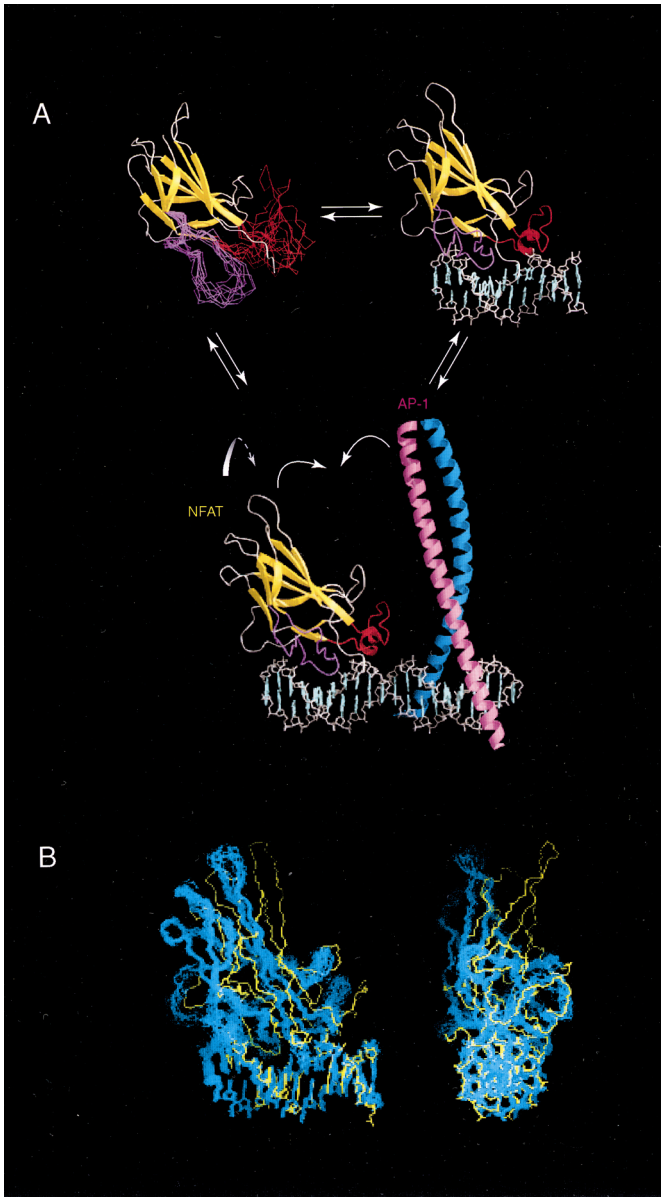

Fig. 2. Induced structural changes accompanying DNA interaction by NFATC1-DBD. (A, top left) NMR-derived solution structure of NFATC1-DBD in the unliganded state (Wolfe et al. 1997) highlighting the disorder in the DNA recognition loop (shown in magenta) and RIR (red) by the use of the ensemble of NMR-derived structures for those parts of the protein. (A, top right) NMR-derived solution structure of the NFATC1–DBD–DNA complex (Zhou et al. 1998) in which the DNA recognition loop and RIR become ordered, including formation of an α-helix. (A, middle) Model built from the NFATC1 DBD–DNA complex solution structure and the X-ray crystallographic structure of the AP-1 bZIP domain (Glover and Harrison 1994), with orientation based on the results of affinity cleavage experiments (Chen et al. 1995). Arrows show the direction that the NFATC1 DBD and AP-1 domains must move to adopt the positions observed in the X-ray crystallographic structure of the ternary NFATC2–AP-1–DNA complex (Chen et al. 1998). (B) Comparison of the NFATC1 DBD–DNA solution structure (blue) (Zhou et al. 1998) with the corresponding portion of the NFATC2–AP-1–DNA X-ray crystallographic structure (yellow) (Chen et al. 1998). This figure was reproduced with permission from Cell.

with more than one base. The broad line widths and low intensities of Lys-26, Lys-29, and Lys-87 side-chain signals in the NMR spectra of the zf1–3–DNA complex indicate that the conformational fluctuations of these lysine side chains occur on a microsecond–millisecond time scale.

Faster conformational averaging of the side chain of Lys-92 in finger 3 is evidenced by the presence of NOEs between its Cδ and Cε protons and bases of both G3 and T26 on opposite DNA strands. Lys-92 hydrogen bonds with several different bases among the ensemble of NMR-derived structures, but its importance is confirmed by severe abrogation of DNA binding affinity upon mutation of Lys-92 to alanine.

Whereas the NMR evidence suggests flexibility in the TFIIIA–DNA interface, the base contact residues display discrete conformations in the crystal structures of Tramtrack, Zif268, and Gli zinc finger protein complexes with DNA (Fairall et al. 1993; Pavletich and Pabo 1991, 1993). Whether this contrast arises from a real difference in the behaviour of the zif1–3–DNA complex or from differences between NMR-derived data and X-ray diffraction derived data is unclear.

lac repressor headpiece

Kaptein and coworkers determined solution structures of *lac* repressor headpiece residues 1–56 (*lac* HP56) in both free (Slijper et al. 1996) and DNA-bound (Chuprina et al. 1993) states. *lac* HP56 comprises three helices, with the first and second helices forming a helix-turn-helix motif. The structure remains largely unchanged upon binding DNA, with the exception of the loop between helices II and III: its conformation changes significantly to allow two side chains to contact DNA.

The same group subsequently recorded ^{15}N relaxation data for both backbone and side-chain nuclei of free and DNA-bound *lac* HP56 (Slijper et al. 1997). These data depend mainly on the dynamics of the N-H bond vector relative to the external magnetic field and reflect both global Brownian rotational tumbling of the molecule–complex and the presence of local internal mobility. The most significant change in backbone ^{15}N dynamics between free and DNA-bound *lac* HP56 occurs in the loop between helices II and III: the entire loop loses its flexibility in the DNA complex, most probably owing to His-29 contacts with DNA.

Side-chain ^{15}N-^{1}H bond vector dynamics should provide a deeper understanding of the protein–DNA interface because asparagine, glutamine, arginine, and lysine are important for protein–DNA binding. The ^{15}N relaxation parameters indicate that two of the DNA-contacting side chains (Gln-18 and Arg-22) exhibit a significant loss of mobility in the DNA complex relative to free HP56. In contrast, the side chains of Gln-26, Asn-50, and Arg-51 remain highly mobile.

The DNA-contacting side chains of Gln-18, Arg-22, and Arg-25 show evidence of intermediate time-scale chemical

exchange in the HP56–DNA complex. This suggests that these residues undergo time-dependent fluctuations between multiple hydrogen bonding interactions. Evidence for such multiple hydrogen bonds was found in both the ensemble of NMR-derived structures and in a restrained molecular dynamics simulation of the HP56–DNA complex (Chuprina et al. 1993).

Trp repressor

Further evidence of the dynamic nature of protein–DNA interfaces was provided by NMR studies of the ternary complex between the *trp* repressor homodimer, the *trp* operator, and the corepressor, L-tryptophan. ^{13}C- and ^{15}N-labelled L-tryptophan was used to determine the exchange rate for the corepressor ligand (Lee et al. 1995). While the ternary complex has a lifetime on the order of minutes, the corepressor exchanges in and out of the protein–DNA complex on a millisecond time scale. Ligand exchange is very likely the mechanism by which the repressor senses and rapidly responds to changes in the cellular concentration of tryptophan. Since the ligand is buried within the protein–DNA complex with contacts to both the protein and DNA, there must be significant movement or "breathing" of one or both of the macromolecules to allow the corepressor to exchange. This is supported by the fact that amide protons in the helix-turn-helix motif (which form one side of the corepressor-binding pocket) undergo rapid hydrogen exchange even in the ternary complex (Zhang et al. 1994).

Ets-1

The DNA-binding domain of Ets-1, the ETS domain, is a member of the winged helix-turn-helix superfamily of DBDs (Donaldson et al. 1996). The ETS domain has several conserved arginine side chains, positioned at the protein–DNA interface in the ETS–DNA complex, that could not be fully assigned in the protein–DNA complex owing to apparent conformational averaging (Werner et al. 1997). These arginines are known from mutagenesis studies to be crucial for high-affinity DNA binding, and many arginines in the ETS–DNA complex are protected from exchange with bulk solvent, suggesting direct, but probably multiple, interactions with DNA.

The *ets* family also provides an example of cooperativity between polypeptides to enhance DNA binding (Graves 1998). NMR and biochemical studies revealed that helix 4 of Ets-1 negatively regulates DNA binding by packing against helix 1 and two other helices that are N-terminal to the ETS domain (Donaldson et al. 1996). In the crystal structure of the ternary complex of GABPα, a member of the *ets* gene family, GABPβ, and a DNA duplex (Batchelor et al. 1998), the GABPα helix corresponding to helix 4 of Ets-1 does not contact helix 1. It is proposed that GABPβ changes the position of the inhibitory helix to derepress DNA binding (Batchelor et al. 1998).

Myb

The DNA-binding region of Myb comprises three imperfect tandem repeats (R1, R2, and R3), each with a variation of the helix-turn-helix DNA recognition motif (Ogata et al. 1994, 1995). R2 exhibits distinctive behaviour compared with the other repeats: it is much less thermally stable (melting temperature of 43°C compared with 61 and 57°C for R1 and R3) (Sarai et al. 1993) and its proton NMR signals are broader, suggesting that R2 undergoes greater conformational fluctuations on the microsecond to millisecond time scale. The authors ascribe these properties to the presence of a cavity at the centre of the hydrophobic core of R2 (Ogata et al. 1995).

Measurement and analysis of backbone ^{15}N relaxation parameters confirms that R2 undergoes slow conformational fluctuations (Ogata et al. 1996). A mutation that acts to fill the central cavity (V103L) stabilizes the structure of R2 but intriguingly results in reduced DNA-binding activity and transactivation (Ogata et al. 1996). The V103L mutation may hamper the observed reorientation of Trp-95 upon DNA binding and may induce some strain in the Myb–DNA complex. The authors conclude that the packing of the R2 hydrophobic core is optimized for the DNA-bound rather than free protein.

Role of hydration water at the protein–DNA interface

Homeodomain

Both NMR and X-ray crystallography can probe hydration water molecules associated with macromolecules and thereby provide important information in elucidating the role of solvent water in biological recognition processes. Identification of hydration water molecules by NMR depends upon the observation of NOEs between hydrogen nuclei (protons) of a water molecule and hydrogen nuclei of the protein. The NOE intensity has a $1/r^6$ dependence on interproton distance and depends also on a correlation function describing the stochastic modulation of the proton–proton dipole–dipole coupling. This modulation can depend upon the Brownian rotational tumbling of the macromolecule or upon translational diffusion of the coupled spins, for example owing to complex dissociation.

A water molecule resides in a protein hydration site for some time before exchanging between the protein site and bulk solvent. The sign and intensity of protein–water NOEs are related to the rate of exchange between bulk solvent and macromolecular hydration site, and thereby give an idea of the residence time of a particular water proton in a particular hydration site. Lifetimes are typically less than 1 ns on a molecular surface and exceed 1 ns in a protein interior or surface cavity. X-ray crystallography provides information on the total fraction of time for which a hydration site is occupied but does not indicate the duration of individual visits to a hydration site. NMR spectroscopy and X-ray crystallography therefore provide complementary data on macromolecular hydration.

Wüthrich and colleagues determined the structure of the complex between a mutant *Antennapedia* homeodomain (Cys-39 replaced by Ser) and a 14 base pair DNA duplex (Billeter et al. 1993). The homeodomain includes a helix-turn-helix DNA-binding motif with the recognition helix in the major groove. An N-terminal arm of the homeodomain contacts the minor groove. Crystal structures of DNA complexes involving homologous homeodomains

Fig. 3. Schematic representations of the multidomain transcription factors discussed in the text: *Saccharomyces cerevisiae* TFIIS, human TFIIB, and TFIIIA from *Xenopus laevis* oocytes.

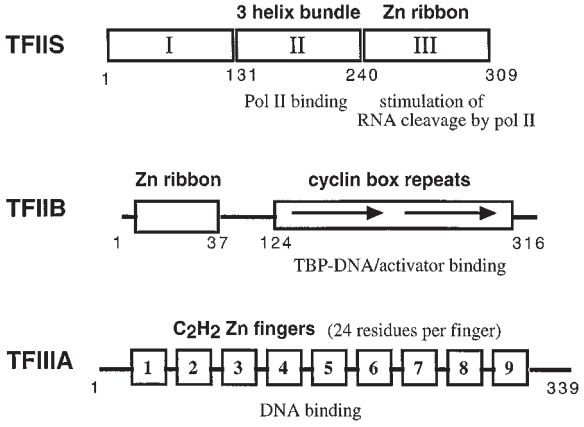

display very similar overall characteristics (Kissinger et al. 1990; Wolberger et al. 1991).

In a subsequent study of hydration water and its role in homeodomain–DNA interaction (Qian et al. 1993*c*; Wüthrich 1993), 39 hydration sites were identified in a cavity at the protein – nucleic acid interface with residence times between 1 ns and 20 ms. In any one NMR-derived conformer, the interfacial cavity contains 1–5 water molecules occupying different positions. The water molecule locations are therefore not precisely defined.

The envelope defined by the 39 hydration sites encompasses most of the homeodomain recognition helix. For two of the residues in the recognition helix, Gln-50 (functionally important) and Asn-51 (strictly conserved), hydrogen bonding with the DNA bases is sterically unfavourable unless mediated by water molecules. Since the residence times of individual water molecules at the protein–DNA interface are below 20 ms, and the water locations are apparently nonspecific, it seems that Gln-50 and Asn-51 make transient, water-mediated hydrogen bonds with multiple bases. Furthermore, experimental NMR evidence has been obtained for millisecond time-scale motion of the side chain of Asn-51 in the *Antp*(*C39S*)–DNA complex (Billeter et al. 1993; Qian et al. 1993*c*). Water-mediated hydrogen bonding has also been observed in crystal structures of DNA complexes with the paired homeodomain (Wilson et al. 1995) and the even-skipped homeodomain (Hirsch and Aggarwal 1995).

One drawback of the exchange rate information available by NMR is that it does not provide precise values for water molecule residence times but rather gives bounds that may range over several orders of magnitude. To address this problem, a 2-ns molecular dynamics simulation in explicit solvent water of an *Antennapedia* homeodomain–DNA complex was carried out (Billeter et al. 1995). This simulation indicates that the water residence times at the protein–DNA interface are closer to the lower bound obtained from the results of NMR experiments (i.e., closer to nanoseconds than milliseconds). The simulation also confirms the possibility of water-mediated hydrogen bonds between Gln-50, Asn-51, and bases and is consistent with a time-dependent ensemble of protein–DNA interactions involving Gln-50 and Asn-51.

NMR analysis of multidomain transcription factors

Most NMR studies of transcription factors have been of small DBDs, which, owing to their size and modular nature, can be readily amenable to NMR analysis. There are often cases, however, in which two or more domains of a protein are needed for biological activity, even though these domains may fold independently of one another. The general transcription factors TFIIS, TFIIB, and TFIIIA are three such proteins (Fig. 3). Recent NMR structural and especially dynamics studies have provided important insights into the biochemical mechanisms of these multidomain proteins.

TFIIS

Transcription elongation factor TFIIS binds to arrested RNA polymerase II elongation complexes and stimulates an endoribonucleolytic cleavage activity in the polymerase that realigns the active site of polymerase with the newly generated 3′ end of the nascent RNA transcript, allowing transcription elongation to continue. TFIIS comprises three structural domains (I–III) (Morin et al. 1996). Domain II of TFIIS contains a 3-helix bundle responsible for binding to RNA polymerase II, followed by two small flexible helices (Morin et al. 1996). Domain III contains a flexible linker followed by a Zn-ribbon (Qian et al. 1993*a*, 1993*b*), a structural motif also found in TFIIB (Zhu et al. 1996). Only protein constructs that contain both domains II and III are active for stimulation of transcription elongation; domains II and III are inactive either individually or in noncovalent combination. Furthermore, mutations at the junction between domains II and III can abrogate elongation activity, suggesting an important role for the region linking the two domains. Olmsted and coworkers used NMR chemical shift, NOE, and relaxation data for transcriptionally active wild-type and mutant yeast TFIIS to show that the 3-helix bundle and Zn-ribbon domains are structurally independent modules linked by the C-terminal portion of domain II and the N-terminal portion of domain III (Olmsted et al. 1998). Although the linker residues do not have a defined tertiary structure and only a small amount of helical secondary structure, they are just as susceptible to inactivating mutations as the 3-helix bundle or the Zn-ribbon regions. The NMR data combined with site-directed mutagenesis suggest a mechanism in which a specific conformation of the linker region is induced upon interaction of TFIIS with the elongation complex but an initial degree of flexibility is required to fit together the ternary elongation complex (Olmsted et al. 1998).

TFIIB

TFIIB is an essential factor for initiation of transcription of protein-coding genes by RNA polymerase II. Human TFIIB is a 316-residue polypeptide (Ha et al. 1991; Malik et al. 1991) comprising two structured domains: residues 106–316 form a protease-resistant core domain (TFIIBc) (Barberis et al. 1993; Malik et al. 1993) and the N-terminal 60 residues form a putative zinc-binding domain (TFIIBn)

that in the *Pyrococcus furiosus* homologue of TFIIB adopts a TFIIS-like zinc ribbon fold (Zhu et al. 1996). TFIIBc is sufficient for binding of TFIIB to its TATA box binding protein–DNA target but TFIIBn is essential for subsequent steps in assembly of a functional transcription initiation complex. The three-dimensional structure of TFIIBc has been determined by NMR spectroscopy and comprises two internally repeated motifs, each with five α-helices arranged as in the cyclin box (Bagby et al. 1995). Compared with the crystal structure of TFIIBc in complex with TBP and a TATA-containing oligonucleotide (Nikolov et al. 1995), the NMR-derived solution structure of free TFIIBc is more compact, with a different repeat-repeat orientation and a significantly shorter first helix in the second repeat. Analysis of backbone ^{15}N relaxation parameters indicates the presence of relatively large amplitude, nanosecond time-scale motions in the TFIIBc interrepeat linker and structural fluctuations throughout the backbone (Hayashi et al. 1998). Interaction of TFIIBc with the acidic activation domain of VP16 or with TFIIBn induces ^{1}H-^{15}N chemical shift and line-width changes concentrated in the first repeat, the interrepeat linker, and the first helix of the second repeat. These results suggest that TFIIB is somewhat pliable and that the conformation of the C-terminal core domain can be modulated by interaction with the N-terminal zinc-binding domain.

TFIIIA

TFIIIA was mentioned above with respect to conformational fluctuations at the protein–DNA interface. Another prominent feature of the zf1–3–DNA complex is the occurrence of extensive contacts between zinc fingers (Foster et al. 1997). The average conformation of unbound zf1–3 is elongated, with flexibility in the interfinger linkers such that the three fingers are essentially independent of one another (Brüschweiler et al. 1995). Comparison of backbone ^{15}N relaxation parameters for free and DNA-bound zf1–3 shows that the backbone mobility of the linker residues is attenuated upon binding DNA, consistent with the substantial packing interactions between the DNA-bound fingers involving both linker and finger residues. The importance of linker residues for DNA-binding affinity had been indicated previously by mutation studies (Thukral et al. 1991; Wilson et al. 1992). Packing interactions between zinc fingers contribute to binding affinity and influence orientation of the domains within the major groove.

Long-range structural restraints

Three novel NMR methodologies have been reported recently for obtaining long-range structural restraints, independent of more conventional sources of structural information available from NMR spectra such as the NOE and scalar coupling constants, both intrinsically short range. One of the novel techniques relies upon the dependence of ^{15}N transverse and longitudinal relaxation rates on the anisotropy of rotational diffusion for nonspherical molecules. This particular method is restricted by the requirement that the diffusion anisotropy exceeds 1.5.

The rotational anisotropy method has been applied to zf1–3 from TFIIIA (the structure and dynamics of the zf1–3–DNA complex were discussed above) to probe the relative orientations and mobilities of the three zinc finger domains (Brüschweiler et al. 1995). Rotational anisotropy analysis indicated that the first three zinc fingers of TFIIIA adopt an average solution conformation that is elongated. The rotational diffusion of zf1–3 is much slower than expected for a single zinc finger, indicating restricted motion of the zinc finger domains relative to one another. A single-residue linker mutation that results in reduced DNA-binding affinity also promotes increased linker flexibility, supporting the hypothesis that motional restriction imposed by the interfinger linkers is important in reducing the entropic price of zf1–3 interaction with DNA (Brüschweiler et al. 1995; Foster et al. 1997).

More recently, the dependence of heteronuclear relaxation rates on rotational diffusion anisotropy has been used to provide input data for simulated annealing calculation of three-dimensional protein structure (Tjandra et al. 1997*a*). In addition to nonspherical proteins, this method is potentially very useful for determining nucleic acid structure.

The second NMR method for obtaining long-range structural constraints relies on measurement of residual dipolar couplings in magnetically oriented molecules. In isotropic solution, dipolar couplings have been largely neglected on the assumption that the couplings average to zero owing to rotational diffusion. Dipolar couplings, however, have a small, nonzero value for molecules with a nonzero magnetic susceptibility anisotropy owing to a small degree of alignment with the magnetic field. The couplings vary with the square of the magnetic field (Gayathri et al. 1982) and are sensitive to the relative orientation of the internuclear vector and molecular magnetic susceptibility tensor. Alternatively and perhaps more generally than depending on a sufficiently large molecular magnetic susceptibility anisotropy, a tunable degree of solute alignment with the magnetic field can be introduced by dissolving macromolecules in a medium containing magnetically oriented particles (Tjandra and Bax 1997).

Bax and colleagues (Tjandra et al. 1997*b*) measured the small residual one-bond ^{15}N-^{1}H and ^{13}C-^{1}H dipolar couplings for the DBD of the erythroid-specific transcription factor GATA-1 in complex with its cognate 16 base pair DNA fragment. Incorporation of dipolar coupling restraints into the simulated annealing protocol for structure calculation results mostly in small local structural changes compared with the original GATA-1–DNA complex structure (Omichinski et al. 1993). The percentage of residues in the most favourable region of the Ramachandran map and the number of bad contacts are, however, improved significantly by the inclusion of dipolar coupling restraints (Tjandra et al. 1997*b*). The loop between strands β3 and β4 of GATA-1 undergoes a large displacement when dipolar couplings are taken into account. There are no long-range NOEs involving the residues in this loop. Dipolar coupling restraints introduce new long-range structural information to define the loop orientation relative to the rest of the polypeptide. ^{15}N relaxation analysis indicates that the loop has low mobility, such that the lack of long-range NOEs does not in this case reflect enhanced mobility/conformational fluctuations on a picosecond–nanosecond time scale. Motional averaging on a microsecond time scale can also be ruled out as the cause of the change in loop orientation because the dipolar couplings

for the loop residues are larger than predicted from the original structure or have opposite sign.

Nucleic acid constitutes a good test system for the use of dipolar coupling restraints because the stacked aromatic groups of the bases lead to a relatively large magnetic susceptibility anisotropy. In contrast, the aromatic side chains and peptide groups that dominate the magnetic susceptibility of most diamagnetic proteins are arranged such that their magnetic susceptibility anisotropy tensors are not collinear. The resultant overall magnetic susceptibility anisotropy tensor is therefore small and hence the potential importance of using a medium such as a dilute aqueous liquid crystalline phase containing magnetically oriented particles (Tjandra and Bax 1997). For protein–DNA complexes in general, the major advantage obtained through introduction of dipolar coupling restraints is in definition of the protein orientation relative to the DNA long axis. Since the dipolar couplings scale with the square of the magnetic field strength, the ongoing progression in magnetic fields to 800 MHz ^{1}H frequency and beyond will extend the number of systems to which dipolar coupling measurements can be usefully applied.

As mentioned above, molecules with a nonzero magnetic susceptibility anisotropy align with the static magnetic field. In addition to nonzero dipolar couplings, this effect causes incomplete averaging of the chemical shift anisotropy component of the Hamiltonian. The degree of alignment is proportional to the square of the static field strength, and therefore chemical shifts should show a magnetic field strength dependence. Like residual dipolar couplings, field-dependent chemical shifts contain information on the orientation of the relevant tensor relative to the molecular magnetic susceptibility tensor and hence are a potential source of long-range structural restraints. Field dependence of chemical shifts is technically difficult to measure accurately, however, since the small effects are easily veiled by chemical shift changes owing to slight sample temperature changes.

Bax and colleagues reported the first measurement of field-dependent chemical shifts in solution (Ottiger et al. 1997). The test system was again the complex between the DNA-binding domain of GATA-1 and a 16 base pair DNA fragment. The field-dependent ^{15}N chemical shifts (Ottiger et al. 1997) are in good agreement with the GATA-1–DNA complex structure refined using dipolar coupling restraints (Tjandra et al. 1997*b*).

Conclusions

The foregoing discussion illustrates the versatility of NMR spectroscopy and particularly its capacity to provide both atomic spatial resolution and temporal resolution over a wide range of frequencies. NMR studies have revealed a common theme of dynamic conformational fluctuations at protein–DNA interfaces, in contrast to the earlier established perception of discrete, well-defined contacts between protein side chains and nucleic acid bases. Conformational malleability of protein–DNA interfaces may arise owing to the thermodynamic advantage that flexibility confers on molecular recognition processes. The entropic cost of conformational restriction of a lysine side chain, for example, is approximately 3 kcal/mol (1 cal = 4.1868 J) (Doig and Sternberg 1995). Similar considerations apply to other types of macromolecular interfaces, as evidenced by the direct demonstration by NMR of flexibility in a protein–peptide interface (Pascal et al. 1995). The newly exploited sources of structural information discussed in the final section of this review demonstrate the vigour of the solution biomolecular NMR field in working towards increased complexity of the molecular systems that can be studied successfully.

Acknowledgements

We thank Professor Gerhard Wagner for supplying Fig. 2, Kyoko Yap for assistance with Fig. 1, and Dingjiang Liu for useful discussions. C.H.A. acknowledges the Medical Research Council (MRC) of Canada, the National Cancer Institute of Canada, and the Cancer Research Society Inc., and M.I. acknowledges the MRC, for financial support of transcription factor research. C.H.A. is an MRC Research Scholar and M.I. is an MRC Scientist and Howard Hughes Medical Institute International Research Scholar.

References

Arrowsmith, C., Pachter, R., Altman, R., and Jardetzky, O. 1991. The solution structures of *Escherichia coli* Trp repressor and Trp aporepressor at an intermediate resolution. Eur. J. Biochem. **202**: 53–66.

Bagby, S., Kim, S., Maldonado, E., Tong, K.I., Reinberg, D., and Ikura, M. 1995. Solution structure of the C-terminal core domain of human TFIIB: similarity to cyclin A and interaction with TATA-binding protein. Cell, **82**: 857–867.

Baleja, J.D., Marmorstein, R., Harrison, S.C., and Wagner, G. 1992. Solution structure of the DNA-binding domain of Cd_2-GAL4 from *S. cerevisiae*. Nature (London), **356**: 450–453.

Barberis, A., Müller, C.W., Harrison, S.C., and Ptashne, M. 1993. Delineation of two functional regions of transcription factor TFIIB. Proc. Natl. Acad. Sci. U.S.A. **90**: 5628–5632.

Batchelor, A.H., Piper, D.E., Charles de la Brousse, F., McKnight, S.L., and Wolberger, C. 1998. The structure of GABPα/β: an ETS domain ankyrin repeat heterodimer bound to DNA. Science (Washington, D.C.), **279**: 1037–1041.

Billeter, M., Qian, Y.Q., Otting, G., Müller, M., Gehring, W., and Wüthrich, K. 1993. Determination of the nuclear magnetic resonance solution structure of an *Antennapedia* homeodomain–DNA complex. J. Mol. Biol. **234**: 1084–1097.

Billeter, M., Güntert, P., Luginbühl, P., and Wüthrich, K. 1995. Hydration and DNA recognition by homeodomains. Cell, **85**: 1057–1065.

Brüschweiler, R., Liao, X., and Wright, P.E. 1995. Long-range motional restrictions in a multidomain zinc-finger protein from anisotropic tumbling. Science (Washington, D.C.), **268**: 886–889.

Chen, L., Oakley, M.G., Glover, J.N.M., Jain, J., Dervan, P.B., Hogan, P.G., Rao, A., and Verdine, G.L. 1995. Only one of the two DNA-bound orientations of AP-1 found in solution cooperates with NFATp. Curr. Biol. **5**: 882–889.

Chen, L., Glover, J.N.M., Hogan, P.G., Rao, A., and Harrison, S.C. 1998. X-ray structure of the NFATp/AP-1/DNA complex. Nature (London), **392**: 42–48.

Cho, H.S., Liu, C.W., Damberger, F.F., Pelton, J.G., Nelson, H.C., and Wemmer, D.E. 1996. Yeast heat shock transcription factor N-terminal activation domains are unstructured as probed by heteronuclear NMR spectroscopy. Protein Sci. **5**: 262–269.

Chuprina, V.P., Rullmann, J.A.C., Lamerichs, R.M.J.N., van Boom, J.H., Boelens, R., and Kaptein, R. 1993. Structure of the complex of *lac* repressor headpiece and an 11 base-pair half-operator by nuclear magnetic resonance spectroscopy and restrained molecular dynamics. J. Mol. Biol. **234**: 446–462.

Dahlman-Wright, K., Baumann, H., McEwan, I.J., Almlof, T., Wright, A.P.H., Gustafsson, J.-A., and Härd, T. 1995. Structural characterization of a minimal functional transactivation domain from the human glucocorticoid receptor. Proc. Natl. Acad. Sci. U.S.A. **92**: 1699–1703.

Doig, A.J., and Sternberg, M.J.E. 1995. Side-chain conformational entropy in protein folding. Protein Sci. **4**: 2247–2251.

Donaldson, L., and Capone, J.P. 1992. Purification and characterization of the carboxy-terminal transactivation domain of Vmw65 from herpes simplex virus type 1. J. Biol. Chem. **267**: 1411–1414.

Donaldson, L.J., Petersen, J.M., Graves, B.J., and McIntosh, L.P. 1996. Solution structure of the ETS domain from murine Ets-1: a winged helix-turn-helix DNA binding motif. EMBO J. **15**: 125–134.

Ellenberger, T.E., Brandl, C.J., Struhl, K., and Harrison, S.C. 1992. The GCN4 basic region leucine zipper binds DNA as a dimer of uninterrupted alpha helices: crystal structure of the protein–DNA complex. Cell, **71**: 1223–1237.

Fairall, L., Schwabe, J.W.R., Chapman, L., Finch, J.T., and Rhodes, D. 1993. The crystal structure of a two zinc-finger peptide reveals an extension to the rules for zinc-finger/DNA recognition. Nature (London), **366**: 483–487.

Foster, M.P., Wuttke, D.S., Radhakrishnan, I., Case, D.A., Gottesfeld, J.M., and Wright, P.E. 1997. Domain packing and dynamics in the DNA complex of the N-terminal zinc fingers of TFIIIA. Nat. Struct. Biol. **4**: 605–608.

Gayathri, C., Bothner-By, A.A., van Zijl, P.C.M., and MacClean, C. 1982. Dipolar magnetic field effects in NMR spectra of liquids. Chem. Phys. Lett. **87**: 192–196.

Ginsberg, A.M., King, B.O., and Roeder, R.G. 1984. Xenopus 5S gene transcription factor, TFIIIA: characterization of a cDNA clone and measurement of RNA levels throughout development. Cell, **39**: 479–489.

Glover, J.N.M., and Harrison, S.C. 1994. The crystal structure of the heterodimeric bZip transcription factor cFos:cJun bound to DNA. Nature (London), **373**: 257–261.

Graves, B.J. 1998. Inner workings of a transcription factor partnership. Science (Washington, D.C.), **279**: 1000–1002.

Ha, I., Lane, W.S., and Reinberg, D. 1991. Cloning of a human gene encoding the general transcription initiation factor IIB. Nature (London), **352**: 689–695.

Härd, T., Kellenbach, E., Boelens, R., Maler, B.A., Dahlman, K., Freedman, L.P., Carlstedt-Duke, J., Yamamoto, K.R., Gustafson, J.-A., and Kaptein, R. 1990. Solution structure of the glucocorticoid receptor DNA-binding domain. Science (Washington, D.C.), **249**: 157–160.

Hayashi, F., Ishima, R., Liu, D., Tong, K.I., Kim, S., Reinberg, D., Bagby, S., and Ikura, M. 1998. Human general transcription factor TFIIB: conformational variability and interaction with VP16 activation domain. Biochemistry, **37**: 7941–7951.

Hirsch, J.A., and Aggarwal, A.K. 1995. Structure of the even-skipped homeodomain complexed to AT-rich DNA: new perspectives on homeodomain specificity. EMBO J. **14**: 6280–6291.

Huth, J.R., Bewley, C.A., Nissen, M.A., Evans, J.N.S., Reeves, R., Gronenborn, A.M., and Clore, G.M. 1997. The solution structure of an HMG-I(Y)-DNA complex defines a new architectural minor groove binding motif. Nat. Struct. Biol. **4**: 657–664.

Kissinger, C.R., Liu, B., Martin-Blanco, E., Kornberg, T.B., and Pabo, C.O. 1990. Crystal structure of an engrailed homeodomain/DNA complex at 2.8 Å resolution: a framework for understanding homeodomain/DNA interactions. Cell, **63**: 579–590.

Kraulis, P. 1991. MOLSCRIPT: a program to produce both detailed and schematic plots of protein structures. J. Appl. Crystallogr. **24**: 946–950.

Kraulis, P.J., Raine, A.R.C., Gadhavi, P.L., and Laue, E.D. 1992. Structure of the DNA-binding domain of zinc GAL4. Nature (London), **356**: 448–450.

Lee, W.T., Revington, M., Farrow, N., Nakomura, A., Utsunomiya-Tate, N., Miyake,Y., Kainosho, M., and Arrowsmith, C.H. 1995. Rapid corepressor exchange from the Trp-repressor/operator complex: an NMR study of [ul-13C/15N]-L-tryptophan. J. Biomol. NMR, **5**: 367–375.

Lefstin, J., and Yamamoto, K.R. 1998. Allosteric effects of DNA on transcriptional regulators. Nature (London), **392**: 885–888.

Lienhard Schmitz, M., dos Santos Silva, M., Altmann, H., Czisch, M., Holak, T., and Baeuerle, P.A. 1994. Structural and functional analysis of the NF-kappa B p65 C-terminus. An acidic and modular transactivation domain with the potential to adopt an alpha-helical conformation. J. Biol. Chem. **269**: 25 613 – 25 620.

Liu, D., Ishima, R., Tong, K.I., Bagby, S., Kokubo, T., Muhandiram, D.R., Kay, L.E., Nakatani, Y., and Ikura, M. 1998. Solution structure of a TBP-TAF_{II}230 complex: protein mimicry of the minor groove surface of the TATA box unwound by TBP. Cell, **94**: 573–583.

Love, J.J., Li, X., Case, D.A., Giese, K., Grosschedl, R., and Wright, P.E. 1995. Structural basis for DNA bending by the architectural transcription factor LEF-1. Nature (London), **376**: 791–795.

Luisi, B.F., Xu, W.X., Otwinowski, Z., Freedman, L.P., Yamamoto, K.R., and Sigler, P.B. 1991. Crystallographic analysis of the interaction of the glucocorticoid receptor with DNA. Nature (London), **352**: 497–505.

Malik, S., Hisatake, K., Sumimoto, H., Horikoshi, M., and Roeder, R.G. 1991. Sequence of general transcription factor TFIIB and relationships to other initiation factors. Proc. Natl. Acad. Sci. U.S.A. **88**: 9553–9557.

Malik, S., Lee, D.K., and Roeder, R.G. 1993. Potential RNA polymerase II-induced interactions of transcription factor TFIIB. Mol. Cell. Biol. **13**: 6253–6259.

Marmorstein, R., Carey, M., Ptashne, M., and Harrison, S.C. 1992. DNA recognition by GAL4: structure of a protein–DNA complex. Nature (London), **356**: 408–414.

McEwan, I.J., Dahlman-Wright, K., Ford, J., and Wright, A.P.H. 1996. Functional interaction of the c-Myc transactivation domain with the TATA binding protein: evidence for an induced fit model of transactivation domain folding. Biochemistry, **35**: 9584–9593.

Merritt, E.A., and Bacon, D.J. 1997. Raster3D photorealistic molecular graphics. Methods Enzymol. **277**: 503–524.

Miller, J., McLachlan, A.D., and Klug, A. 1985. Repetitive zinc-binding domains in the protein transcription factor IIIA from Xenopus oocytes. EMBO J. **4**: 1609–1614.

Morin, P., Awrey, D., Edwards, A.M., and Arrowsmith, C. 1996. Elongation factor TFIIS contains three structural domains: solution structure of domain II. Proc. Natl. Acad. Sci. U.S.A. **93**: 10 604 – 10 608.

Nikolov, D.B., Chen, H., Halay, E.D., Usheva, A.A., Hisatake, K., Lee, D.K., Roeder, R.G., and Burley, S.K. 1995. Crystal structure of a TFIIB-TBP-TATA-element ternary complex. Nature (London), **377**: 119–128.

Ogata, K., Kanei-Ishii, C., Sasaki, M., Hatanaka, H., Nagadoi, A., Enari, M., Nakamura, H., Nishimura, Y., Ishii, S., and Sarai, A. 1996. The cavity in the hydrophobic core of Myb DNA-binding domain is reserved for DNA recognition and trans-activation. Nat. Struct. Biol. **3**: 178–187.

Ogata, K., Morikawa, S., Nakamura, H., Hojo, H., Yoshimura, S., Zhang, R., Aimoto, S., Ametani, Y., Hirata, Z., Sarai, A., Ishii, S., and Nishimura, Y. 1995. Comparison of the free and DNA-complexed forms of the DNA-binding domain from c-Myb. Nat. Struct. Biol. **2**: 309–319.

Ogata, K., Morikawa, S., Nakamura, H., Sekikawa, A., Inoue, T., Kanai, H., Sarai, A., Ishii, S., and Nishimura, Y. 1994. Solution structure of a specific DNA complex of the Myb DNA-binding domain with cooperative recognition helices. Cell, **79**: 639–648.

Olmsted, V., Awrey, D.E., Koth, C., Morin, P.E., Shan, X., Kazanis, S., Edwards, A.M., and Arrowsmith, C.H. 1998. Yeast transcript elongation factor TFIIS: structure and function I. NMR structural analysis of the minimal transcriptionally active region. J. Biol. Chem. **273**: 22 589 – 22 594.

Omichinski, J.G., Clore, G.M., Schaad, O., Felsenfeld, G., Trainor, C., Appella, E., Stahl, S.J., and Gronenborn, A.M. 1993. NMR structure of a specific DNA complex of Zn-containing DNA binding domain of GATA-1. Science (Washington, D.C.), **261**: 438–446.

Omichinski, J.G., Pedone, P.V., Felsenfeld, G., Gronenborn, A.M., and Clore, G.M. 1997. The solution structure of a specific GAGA factor-DNA complex reveals a modular binding mode. Nat. Struct. Biol. **4**: 122–132.

Ottiger, M., Tjandra, N., and Bax, A. 1997. Magnetic field dependent amide ^{15}N chemical shifts in a protein–DNA complex resulting from magnetic ordering in solution. J. Am. Chem. Soc. **119**: 9825–9830.

Otwinowski, Z., Schevitz, R.W., Zhang, R.-G., Lawson, C.L., Joachimiak, A., Marmorstein, R.Q., Luisi, B., and Sigler, P.B. 1988. Crystal structure of Trp repressor/operator complex at atomic resolution. Nature (London), **335**: 321–329.

Pascal, S.M., Yamazaki, T., Singer, A.U., Kay, L.E., and Forman-Kay, J.D. 1995. Structural and dynamic characterization of the phosphotyrosine binding region of a Src homology 2 domain-phosphopeptide complex by NMR relaxation, proton exchange, and chemical shift approaches. Biochemistry, **34**: 11 353 – 11 362.

Pathak, D., and Sigler, P.B. 1992. Updating structure–function relationships in the bZip family of transcription factors. Curr. Opin. Struct. Biol. **2**: 116–123.

Pavletich, N.P., and Pabo, C.O. 1991. Zinc finger-DNA recognition: crystal structure of a Zif268-DNA complex at 2.1 Å. Science (Washington, D.C.), **252**: 809–817.

Pavletich, N.P., and Pabo, C.O. 1993. Crystal structure of a five-finger GLI-DNA complex: new perspectives on zinc fingers. Science (Washington, D.C.), **261**: 1701–1707.

Qian, Y.Q., Billeter, M., Otting, G., Müller, G., Gehring, W.J., and Wüthrich, K. 1989. The structure of the *Antennapedia* homeodomain determined by NMR spectroscopy in solution: comparison with prokaryotic repressors. Cell, **59**: 573–580.

Qian, X., Gozani, S.N., Yoon, H., Jeon, C., Agarwal, K., and Weiss, M.A. 1993*a*. Novel zinc finger motif in the basal transcriptional machinery: three-dimensional NMR studies of the nucleic acid binding domain of transcriptional elongation factor TFIIS. Biochemistry, **32**: 9944–9959.

Qian, X., Jeon, C., Yoon, H., Agarwal, K., and Weiss, M. 1993*b*. Structure of a new nucleic-acid-binding motif in eukaryotic transcriptional elongation factor TFIIS. Nature (London), **365**: 277–279.

Qian, Y.Q., Otting, G., and Wüthrich, K. 1993*c*. NMR detection of hydration water in the intermolecular interface of a protein–DNA complex. J. Am. Chem. Soc. **115**: 1189–1190.

Radhakrishnan, I., Perez-Alvarado, G.C., Parker, D., Dyson, H.J., Montminy, M.R., and Wright, P.E. 1997. Solution structure of the KIX domain of CBP bound to the transactivation domain of CREB: a model for activator:coactivator interactions. Cell, **91**: 741–752.

Sarai, A., Uedaira, H., Morii, H., Yasukawa, T., Ogata, K., Nishimura, Y., and Ishii, S. 1993. Thermal stability of the DNA-binding domain of the Myb oncoprotein. Biochemistry, **32**: 7759–7764.

Saudek, V., Pasley, H.S., Gibson, T., Gausepohl, H., Frank, R., and Pastore, A. 1991. Solution structure of the basic region from the transcriptional activator GCN4. Biochemistry, **30**: 1310–1317.

Slijper, M., Bonvin, A.M.J.J., Boelens, R., and Kaptein, R. 1996. Refined structure of lac repressor headpiece (1–56) determined by relaxation matrix calculations from 2D and 3D NOE data: change of tertiary structure upon binding to the lac operator. J. Mol. Biol. **259**: 761–773.

Slijper, M., Boelens, R., Davis, A.L., Konings, R.N.H., van der Marel, G.A., van Boom, J.H., and Kaptein, R. 1997. Backbone and side chain dynamics of *lac* repressor headpiece (1–56) and its complex with DNA. Biochemistry, **36**: 249–254.

Spolar, R.S., and Record, M.T., Jr. 1994. Coupling of local folding to site-specific binding of proteins to DNA. Science (Washington, D.C.), **263**: 777–784.

Sun, L.J., Peterson, B.R., and Verdine, G.L. 1997. Dual role of the NFAT insert region in DNA recognition and cooperative contact to AP-1. Proc. Natl. Acad. Sci. U.S.A. **94**: 4919–4924.

Thukral, S.K., Morrison, M.L., and Young, E.T. 1991. Alanine scanning site-directed mutagenesis of the zinc fingers of transcription factor ADR1: residues that contact DNA and that transactivate. Proc. Natl. Acad. Sci. U.S.A. **88**: 9188–9192.

Tjandra, N., and Bax, A. 1997. Direct measurement of distances and angles in biomolecules by NMR in a dilute liquid crystalline medium. Science (Washington, D.C.), **278**: 1111–1114.

Tjandra, N., Garrett, D.S., Gronenborn, A.M., Bax, A., and Clore, G.M. 1997*a*. Defining long range order in NMR structure determination from the dependence of heteronuclear relaxation times on rotational diffusion anisotropy. Nat. Struct. Biol. **4**: 443–449.

Tjandra, N., Omichinski, J.G., Gronenborn, A.M., Clore, G.M., and Bax, A. 1997*b*. Use of dipolar ^{1}H-^{15}N and ^{1}H-^{13}C couplings in the structure determination of magnetically oriented molecules in solution. Nat. Struct. Biol. **4**: 732–738.

Uesugi, M., Nyanguile, O., Lu, H., Levine, A.J., and Verdine, G.L. 1997. Induced α helix in the VP16 activation domain upon binding to a human TAF. Science (Washington, D.C.), **277**: 1310–1313.

Van Hoy, M., Leuther, K.K., Kodadek, T., and Johnston, S.A. 1993. The acidic activation domains of the GCN4 and GAL4 proteins are not α helical but form β sheets. Cell, **72**: 587–594.

Werner, M.H., Huth, J.R., Gronenborn, A.M., and Clore, G.M. 1995. Molecular basis of human 46X,Y sex reversal revealed from the three-dimensional solution structure of the human SRY-DNA complex. Cell, **81**: 705–714.

Werner, M.H., Clore, G.M., Fisher, C.L., Fisher, R.J., Trinh, L., Shiloach, J., and Gronenborn, A.M. 1997. Correction of the NMR structure of the ETS1/DNA complex. J. Biomol. NMR, **10**: 317–328.

Wilson, T.E., Day, M.L., Pexton, T., Padgett, K.A., Johnston, M., and Milbrandt, J. 1992. In vivo mutational analysis of the NGFI-A zinc fingers. J. Biol. Chem. **267**: 3718–3724.

Wilson, D.S., Guenther, B., Desplan, C., and Kuriyan, J. 1995.

High resolution crystal structure of a paired (Pax) class cooperative homeodomain dimer on DNA. Cell, **82**: 709–719.

Wolberger, C., Vershon, A.K., Liu, B., Johnson, A.D., and Pabo, C.O. 1991. Crystal structure of a *MATα2* homeodomain-operator complex suggests a general model for homeodomain–DNA interactions. Cell, **67**: 517–528.

Wolfe, S.A., Zhou, P., Dötsch, V., Chen, L., You, A., Ho, S.N., Crabtree, G.R.,Wagner, G., and Verdine, G. 1997. An unusual Rel-like architecture in the DNA-binding domain of NFATc. Nature (London), **385**: 172–176.

Wüthrich, K. 1993. Hydration of biological macromolecules in solution: surface structure and molecular recognition. Cold Spring Harbor Symp. Quant. Biol. **58**: 149–157.

Zhang, H., Zhao, D., Revington, M., Lee, W., Jia, X., Arrowsmith, C., and Jardetzky, O. 1994. The solution structures of the trp repressor-operator DNA complex. J. Mol. Biol. **238**: 592–614.

Zhao, D., Arrowsmith, C.H., Jia, X., and Jardetzky, O. 1993. Refined solution structures of the *Escherichia coli* trp holo- and aporepressor. J. Mol. Biol. **229**: 735–746.

Zhou, P., Sun, L.J., Dötsch, V., Wagner, G., and Verdine, G.L. 1998. Solution structure of the core NFATC1/DNA complex. Cell, **92**: 687–696.

Zhu, W., Zeng, Q., Colangelo, C. M., Lewis, M., Summers, M.F., and Scott, R.A. 1996. The N-terminal domain of TFIIB from *Pyrococcus furiosus* forms a zinc ribbon. Nat. Struct. Biol. **3**: 122–124.